ELSEVIER

Journal of Volcanology and Geothermal Research 86 (1998) 1–18

Journal of volcanology and geothermal research

Pit crater formation on Kilauea volcano, Hawaii.

Chris H. Okubo [a,*], Stephen J. Martel [b,1]

[a] *Hawaii Institute of Geophysics and Planetology, School of Ocean and Earth Science and Technology, University of Hawaii, HI 96822, USA*

[b] *Department of Geology and Geophysics, School of Ocean and Earth Science and Technology, University of Hawaii, HI 96822, USA*

Received 16 June 1997; accepted 12 May 1998

Abstract

Most of the known pit craters in Hawaii occur along the East and Southwest Rift Zones of Kilauea volcano. The pit craters typically are either astride a single rift zone fracture or between a pair of rift zone fractures. These fractures are prominent in the pit crater walls. The pit craters are elliptical in plan view, with their major diameters ranging from 8 to 1140 m. They range in depth from 6 m to 186 m. They typically develop with initially steep, locally overhanging walls, but as the walls collapse, the craters fill with talus and become shaped like inverted elliptical cones. None of the craters apparently formed as eruptive vents, although some have been subsequently filled by lava. Devil's Throat is the best-exposed pit crater along the East Rift Zone. It is sited at a 'waist' between two east-striking zones of ground cracks; the spacing between the crack zones decreases towards Devil's Throat. East-striking fractures are also prominent in the pit crater walls. Pit craters along the Southwest Rift Zone typically are elongate in plan view along the direction of the rift, have large caves at their bases along the long axes of the craters, and are smaller than those of the East Rift Zone. Some closely spaced pits there have coalesced to form a trough. Based on our observations and mechanical considerations, we infer that pit craters form by stoping over an underlying large-aperture rift zone fracture, and not by piston-like collapse over broad magma bodies or voids. Flow of magma along the underlying fracture may remove stoped blocks and prevent the fracture from being choked with debris. This mechanism is consistent with pit crater location, ground crack patterns, the preferred orientation of fractures in pit crater walls, and pit crater geometry (both in map view and cross-section). The mechanism also fits with observations of stoping into a gaping rift fracture that conducted lava from Kilauea caldera during the 1920s. Additionally, the ratio of pit crater width to depth of 0.5 to 2 is consistent with pit craters forming over a nearly vertical opening mode fracture.

Keywords: pit crater; stoping; rift zone; Kilauea

1. Introduction

''By the term 'pit-crater,' is meant that description of crater of which there is no appearance whatever until one is close upon it, and which never throws out lava. The formation of these might be occasioned by the undermining of the part beneath them. It will be seen, on viewing the map, that some of them have only a small part of their bottom covered with lava. The most probable conjecture, in relation to their origin, that occurred to us while moving over the ground was, that a stream of lava

* Corresponding author. Fax: +1-808-956-6322; E-mail: chriso@pgd.hawaii.edu

[1] Fax: +1-808-956-3188; E-mail: martel@soest.hawaii.edu.

0377-0273/98/$19.00
PII: S0377-0273(98)00070-5

had passed underneath, and running off had left large cavities, into which the superincumbent rock above, not having support, had fallen, and when this had sunk sufficiently low, the lava had flowed in and filled the bottom. Some of these pit-craters are from eight hundred to one thousand feet deep, but none that I saw had the appearance of eruption within themselves.'' From Wilkes (1845).

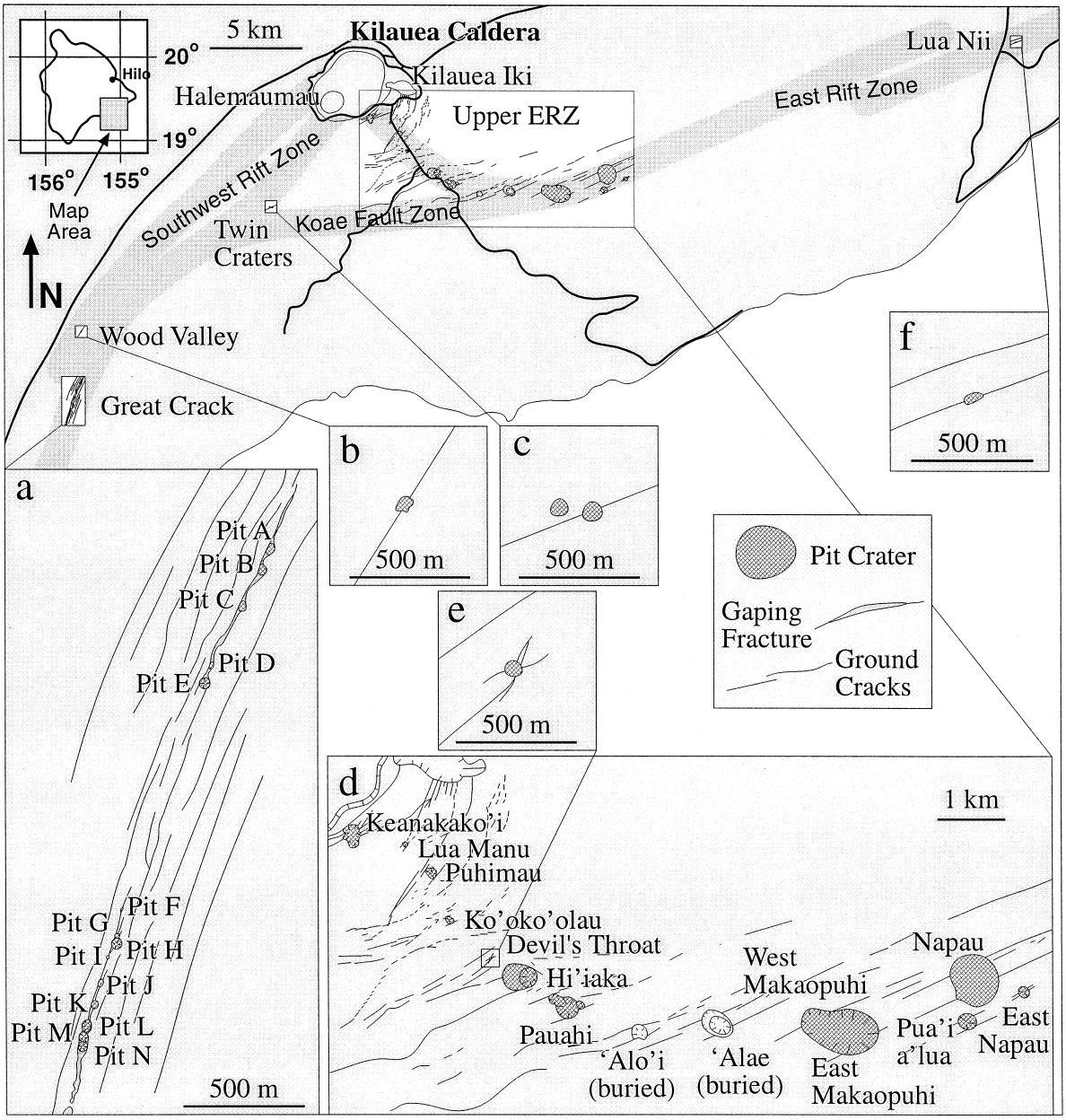

Fig. 1. Pit craters on the East and Southwest Rift Zones of Kilauea volcano. Most pit craters are astride ground crack traces. Ground cracks traces are from aerial photograph interpretation and field inspection. Ground cracks in (d) based on de Saint Ours (1982) and Holcomb (1976). Note the different scales for each figure.

Since Wilkes (1845) proposed the term 'pit crater' to describe the pits along the East Rift Zone (ERZ) of Kilauea volcano, investigators have applied the term to a wide variety of diverse pit-like structures (Halliday, in press), while the origin of the pit craters along the ERZ has attracted little attention. The purpose of this paper is to re-state what we view to be the original intent of the term pit crater and then present field observations and mechanical arguments in support of a model of pit crater formation.

Based on the original definition by Wilkes (1845) of the term and field observations of the pits he describes, we regard pit craters to be elliptical rimless pits, with overhanging, steep, or talus-covered walls within volcanic rock, which have not formed as primary eruptive vents. Additionally, pit craters are not collapsed roof sections of ordinary surficial lava tubes. Pit craters are prominent along volcanic rift zones. Seventeen have been identified along Kilauea's ERZ, and a series of others occurs along the volcano's Southwest Rift (Fig. 1). Neighboring Mauna Loa volcano has ten named rift zone pit craters and Hualalai volcano has five to seven possible rift zone pit craters. Volcan Equador, Galapagos, has four pit craters along its rift zone. Buried pit craters are known to exist along Kilauea's ERZ, as well as along the rift zones of Lana'i, West Maui, East Moloka'i, and Kaua'i volcanoes. Similar pit-like features are also associated with Icelandic rifts (Th. Thordarson, written commun., 1996). Pit craters also appear to exist along the rift zones of martian and venusian volcanoes (e.g., Carr et al., 1977; Senske et al., 1992).

Several models have been proposed for the origin of pit craters. Stearns and Clark (1930) suggested that pit crater formation begins through stoping above a magma-filled fracture, and that after subsidence of the magma, roof collapse occurs in the area of stoping and leads to the formation of a pit crater. Blevins (1981) suggested that pit craters on Kilauea's ERZ are the result of roof collapse over a broad cavity underlying the ERZ. Favre (1993) suggested that some pit craters might form above partially drained dikes. Walker (1988) suggested that pit craters form above void spaces over a deep, long-lived, active conduit that transports magma from the Kilauea summit chamber into the rift zone, the conduit being subhorizontal and cylindrical. Others (e.g., Macdonald et al., 1990; Hirn et al., 1991; Senske et al., 1992) consider that pit craters form as a result of piston-like ground subsidence over a large, depressurized, near-surface magma reservoir. Our study strongly indicates that pit craters form in response to stoping above large, nearly vertical, subsurface rift zone fractures.

We begin by describing the locations and appearance of pit craters on Kilauea. Next we review observations of stoping along the southwest rim of Kilauea caldera in 1922. Based on these collective observations, we present a conceptual model for pit crater formation and then examine some of its key mechanical aspects. Finally we conclude with a discussion of the distribution and size of Kilauea's pit craters.

2. Pit craters of the East Rift Zone of Kilauea

The East Rift pit craters lie on the axis of the ERZ, which is expressed subaerially as a belt 3 km wide and 50 km long. The rift zone is covered with extensive flow fields and is dotted by numerous parasitic shield volcanoes, scoria cones, and pit craters. Most of the ERZ is covered by dense vegetation. The segments along which most of the pit craters are located (Fig. 1d) are known as the Upper East Rift Zone and the Middle East Rift Zone. Proceeding from the edge of Kilauea caldera, the Upper ERZ strikes southeast for 5 km downrift. The ERZ then bends and strikes northeast. The Middle and Lower East Rift Zone segments retain this northeast strike further downrift. Eleven of the seventeen pit craters are located near Kilauea caldera, on the southeast-striking Upper ERZ, while West Makaopuhi, East Makaopuhi, Pua'i 'alua, Napau, and East Napau are located on the northeast-striking Middle ERZ. Lua Nii is located on the Lower ERZ.

The ERZ contains numerous ground cracks that strike northeast (Fig. 1d). Along the Upper ERZ, the ground cracks intersect the rift axis at nearly right angles. On the Middle and Lower ERZ, the ground cracks are nearly parallel with the rift zone axis. In addition, the Koa'e Fault Zone and faults concentric about Kilauea caldera cut through the Upper ERZ. Thus a whole series of structural flaws are evident within the ERZ.

Eruptive fissure vents intersect some East Rift pit craters but not all. Although most pit craters contain ponded lava from intersecting or near-by vents, the absence of radial flows indicates that the pit craters are not primary vents for effusive eruptions. The lack of radial distributions of pyroclastic debris around the pit craters indicates that these pits are also not the primary vents for explosive eruptions, although phreatic explosions may occur within ponded lava erupted from intersecting or near-by vents (e.g., Stearns and Clark, 1930).

The ERZ pit craters range in surface diameter from 20 m to 1140 m and in depth from 23 m to 186 m (Table 1). Pit crater surface diameters can increase over time through wall collapse, and their depths can decrease over time as lava and talus fill the pits.

The pit craters are either shaped like elliptical cylinders or inverted elliptical cones, and commonly are slightly elongate parallel to the strike of the rift zone. Cylindrical pits have steep, unvegetated walls, and their broken rock faces appear fresh, showing little discoloration from weathering. Conical pits, on

Table 1
Known pit craters along Kilauea's East Rift Zone (ERZ) and Southwest Rift Zone (SWRZ)

Pit crater name	Rift zone	Depth (m)	Surface diameter (m)		Center		Known cave?
			Long axis	Short axis	Latitude	Longitude	
Keanakako'i (in 1963)	ERZ	64	486	330	19°24′11″	155°16′06″	No
Lua Manu (in 1963)	ERZ	43	126	90	19°24′06″	155°15′24″	No
Puhimau (in 1963)	ERZ	165	262	180	19°23′47″	155°15′06″	No
Ko'oko'olau (in 1963)	ERZ	30	204	144	19°23′16″	155°14′51″	No
Devil's Throat (in 1998)	ERZ	50	53.5	42.5	19°22′50″	155°14′24″	Yes[b]
Hi'iaka (outer) (in 1963)	ERZ	24	714	546	19°22′39″	155°13′59″	No
Hi'iaka (inner) (in 1963)	ERZ	110	384	378	19°22′39″	155°14′06″	No
North Pauahi (in 1963)	ERZ	165	282	240	19°22′25″	155°13′36″	No
Central Pauahi (in 1963)	ERZ	134	504	378	19°22′18″	155°13′30″	No
East Pauahi (in 1963)	ERZ	49	222	180	19°22′21″	155°13′20″	No
Alo'i (in 1963)	ERZ	70	327	306	19°22′05″	155°12′40″	No
Alae (in 1963)	ERZ	94	672	498	19°22′09″	155°11′45″	No
West Makaopuhi (in 1963)	ERZ	305	732	720	19°22′08″	155°10′36″	No
East Makaopuhi (in 1963)	ERZ	186	1020	990	19°22′05″	155°10′14″	No
Pua'i a'Lua (in 1963)	ERZ	134	372	345	19°22′11″	155°08′51″	No
Napau (in 1963)	ERZ	60	1140	840	19°22′39″	155°08′47″	No
East Napau (in 1963)	ERZ	79	258	198	19°22′29″	155°08′13″	No
Lua Nii (in 1955)	SWRZ	23[c]	27[c]	20[c]	19°26′33″	154°56′43″	Yes[c]
West Twin Crater (in 1966)	SWRZ	85[d]	50[d]	50[d]	19°21′29″	155°19′00″	Yes[d]
East Twin Crater (in 1966)	SWRZ	70[a]	50[d]	50[d]	19°21′30″	155°19′58″	Yes[d]
Wood Valley (in 1998)	SWRZ	33	24	30	19°17′47″	155°24′43″	Yes[a]
Great Crack Pit A (in 1998)	SWRZ	13	37	10	19°16′20″	155°24′44″	Yes
Great Crack Pit B (in 1998)	SWRZ	13	37	27	19°16′17″	155°25′00″	Yes
Great Crack Pit C (in 1998)	SWRZ	28.5	34.5	24	19°16′16″	155°24′47″	Yes
Great Crack Pit D (in 1998)	SWRZ	10	20	10	19°16′13″	155°24′49″	Yes
Great Crack Pit E (in 1998)	SWRZ	20	43	38	19°16′08″	155°24′51″	Yes
Great Crack Pit F (in 1998)	SWRZ	12.5	16	8	19°15′45″	155°25′00″	Yes
Great Crack Pit G (in 1998)	SWRZ	6	12	10	19°15′44″	155°25′01″	Yes
Great Crack Pit H (in 1998)	SWRZ	16	45	25	19°15′43″	155°25′01″	Yes
Great Crack Pit I (in 1998)	SWRZ	10	10	10	19°15′42″	155°25′02″	Yes
Great Crack Pit J (in 1998)	SWRZ	20	30	20	19°15′41″	155°25′03″	No
Great Crack Pit K (in 1998)	SWRZ	15	40	30	19°15′39″	155°25′03″	No
Great Crack Pit L (in 1998)	SWRZ	15	42	38	19°15′37″	155°25′05″	No
Great Crack Pit M (in 1998)	SWRZ	16	40	40	19°15′36″	155°25′05″	No
Great Crack Pit N (in 1998)	SWRZ	14	40	37	19°15′34″	155°25′06″	Yes

[a] From Favre (1993); [b] from Jaggar (1947); [c] from Macdonald and Eaton (1964); [d] from Whitfield (1980).

the other hand, have walls covered partially or totally by talus.

Most pit craters are singular, but some have coalesced. At the Pauahi complex (Fig. 2), three pit craters of various sizes and depths have coalesced, but they remain as individual pits separated by septa. The two Makaopuhi pit craters (Fig. 1d) are almost indistinguishable as separate pits as they share a common floor of ponded lava. The upper remnant of the septum separating the two is barely visible amidst the talus mantling the walls. Ko'oko'olau pit crater (Fig. 1d) could possibly be two coalesced pits; a septum-like ridge is visible in aerial photographs, but heavy vegetation within and around the pit hinders direct ground observation.

Two of the pits appear to be floored by down-dropped sections of the lava flow surface present outside the pit crater rims. East Pauahi is one example (Stearns and Clark, 1930). The sections slope inward toward the center of the 49-m-deep pit, giving it a conical shape. The rim of East Pauahi is defined by an arcuate fracture separating the surrounding flat-lying lavas from the apparently down dropped sections. The second pit, Hi'iaka, apparently contains several down-dropped sections as well (Stearns and Clark, 1930). Hi'iaka has a fault-bounded main pit and, at its eastern boundary, a deep inner pit. The apparently down-dropped sections floor the 24-m-deep main pit, which is elongate parallel to the northeast-striking Koa'e faults. In contrast the inner pit is slightly elongate parallel to the southeast strike of the Upper ERZ.

The most common and distinguishable features near the pit craters are a pair of nearly parallel ground crack zones, which Blevins (1981) termed bounding faults (Fig. 2). These are delineated on aerial photographs by lines of eruptive fissure vents, concentrated vegetation, and ground shadows. Field observations confirm that these crack zones strike northeast–southwest and intersect the northwest and southeast walls of the pit craters. At their intersection with the pit walls, each crack zone extends to the pit floor and is near-vertical, dipping toward the opposite crack zone at angles greater than 80°. The paired ground crack zones strike N 50° E to N 80° E, with the more northerly striking crack zones generally at pit craters closer to Kilauea caldera. The dilation direction of individual ground cracks is perpendicular to the general trend of the ground crack zone.

Some of the East Rift pit craters are sited at a 'waist' between the paired ground crack zones, where the spacing between the crack zones decreases.

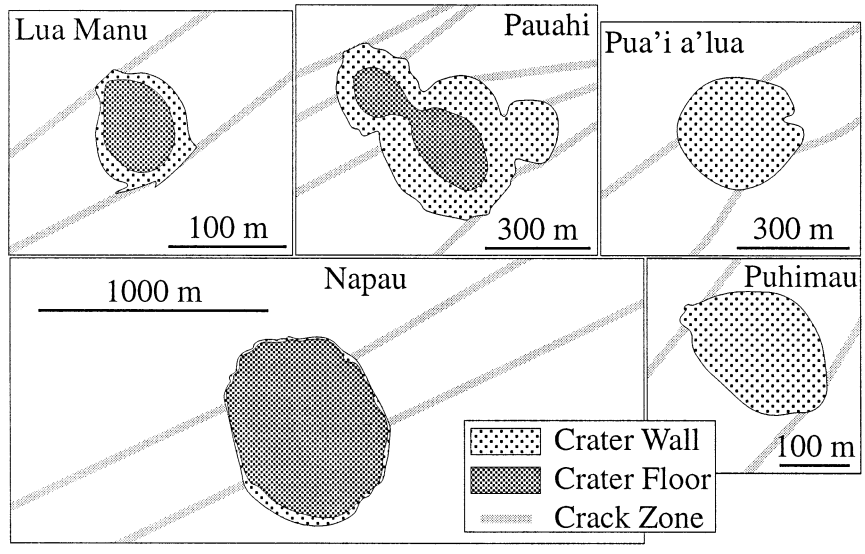

Fig. 2. Representative pit craters from the East Rift Zone of Kilauea volcano with highlighted paired ground crack zones. The majority of Kilauea's pit craters are sited on pairs of ground crack zones recognized in aerial photographs and observed in the field. Note the different scales for each figure.

Ko'oko'lau, Devil's Throat, and Pua'i a'lua provide three examples. 'Alo'i and 'Alae, which were buried during the Mauna Ulu eruptions (1969–1974), were also sited at waists. These waists are visible on 1:6000 scale aerial photographs taken in 1965. The areas surrounding both pit craters in 1965 were sparsely vegetated, and the ground cracks are clearly visible on the photographs. The current absence of a 'waist' in the paired ground crack zones at most of the pit craters is not evidence that a waist was always absent; waists could have been destroyed by collapse of pit walls.

2.1. Initial observations of Devil's Throat and Lua Nii pit craters

Two East Rift pit craters have been observed as, or shortly after, they breached the surface: Devil's Throat and Lua Nii. Devil's Throat, one of the smaller East Rift pit craters, is located on the axis of the Upper ERZ between Ko'oko'lau and Hi'iaka pit craters (Fig. 1d,e). Lua Nii, also a small East Rift Pit crater, is located about 35 km east of Kilauea caldera (Fig. 1f).

In February 1912, Jaggar (1912, 1947) observed Devil's Throat as having a surface opening 11–15 m across leading into a large, cupola-shaped void such that the diameter of the pit increased with depth, which he estimated at 76 m. The entire floor of the void was flat, with no talus at the base of the walls. At the bottom of the void, Jaggar observed a cave within the northwest wall. Devil's Throat was explored on June 23, 1923 by W.T. Sinclair, who measured its depth as 258 ft [78 m] (Scribner and Doerr, 1932). Schribner and Doerr's account does not mention the cave at the base of the pit described by Jaggar.

Macdonald and Eaton (1964) observed Lua Nii as it broke the ground surface on March 20, 1955 when a 7–9-m section of roof collapsed into a larger underground void. Lua Nii opened up along a fissure vent associated with the 1955 eruptions in East Puna, on the Lower ERZ. This particular vent ceased erupting and the eruption had shifted uprift one week before Lua Nii developed. The initial opening of the pit was announced by a sharp explosion and a small puff of black dust. No rock was ever erupted or ejected from the pit, although the fissure itself continued to fume and retained enough heat from the previous week's eruption to apparently remelt the pit's wall rock. Macdonald and Eaton examined the pit crater from the air the next day and estimated the surface opening to be 20 ft [6 m] in diameter and estimated a depth of 50 to 75 ft [15 to 23 m]. The pit was floored with brightly glowing material. The pit ''increased in diameter downward, the walls overhanging 15 to 20 ft [5 to 6 m] on all sides except the southwest, where the chamber extended back at least 50 ft [15 m] beyond the crater rim'' (i.e., along the axis of the rift). The solidified remnant of the feeder dike for the fissure vent was observed in the pit's southwest and northeast walls.

The surface expressions of both pit craters developed in similar manners. After initial openings formed, the surface diameter of the pits increased over time through roof and wall collapse (Macdonald, 1972).

2.2. Present day observations of Devil's Throat

Devil's Throat has grown in surface diameter and decreased in depth since 1912. In February 1912, Devil's Throat was elongate in the direction N 60° E, had surface dimensions of 15 m × 11 m, and was about 76 m deep (Jaggar, 1912). As of February 1998, Devil's Throat is nearly cylindrical, with an average surface diameter of 48 m and a depth of 50 m. This marks a 33–37 m increase in surface diameter and a 26 m decrease in depth over the past 86 yr. The cave at the base of the northwest wall, noted by Jaggar (1912), is no longer visible. Arcuate ground cracks subparallel to the crater rim occur around the circumference and within a meter or two of the pit rim. The greatest concentration occurs near the eastern rim of the pit.

Two informally-named right-lateral faults occur near Devil's Throat (Fig. 3). Both strike N 60° E. 'Bean's Fault' is 110 m northwest of Devil's Throat. Its component en echelon fractures strike roughly east–west and have dilated in a NNE–SSW direction. These fractures typically have trace lengths of 10–20 m and step to the left. The second fault, 'Patty's Fault', intersects the southeast rim of Devil's Throat. From Devil's Throat, segments of Patty's Fault strike northeast for 100 m, and southwest for 150 m; further west they strike east–west. The trace

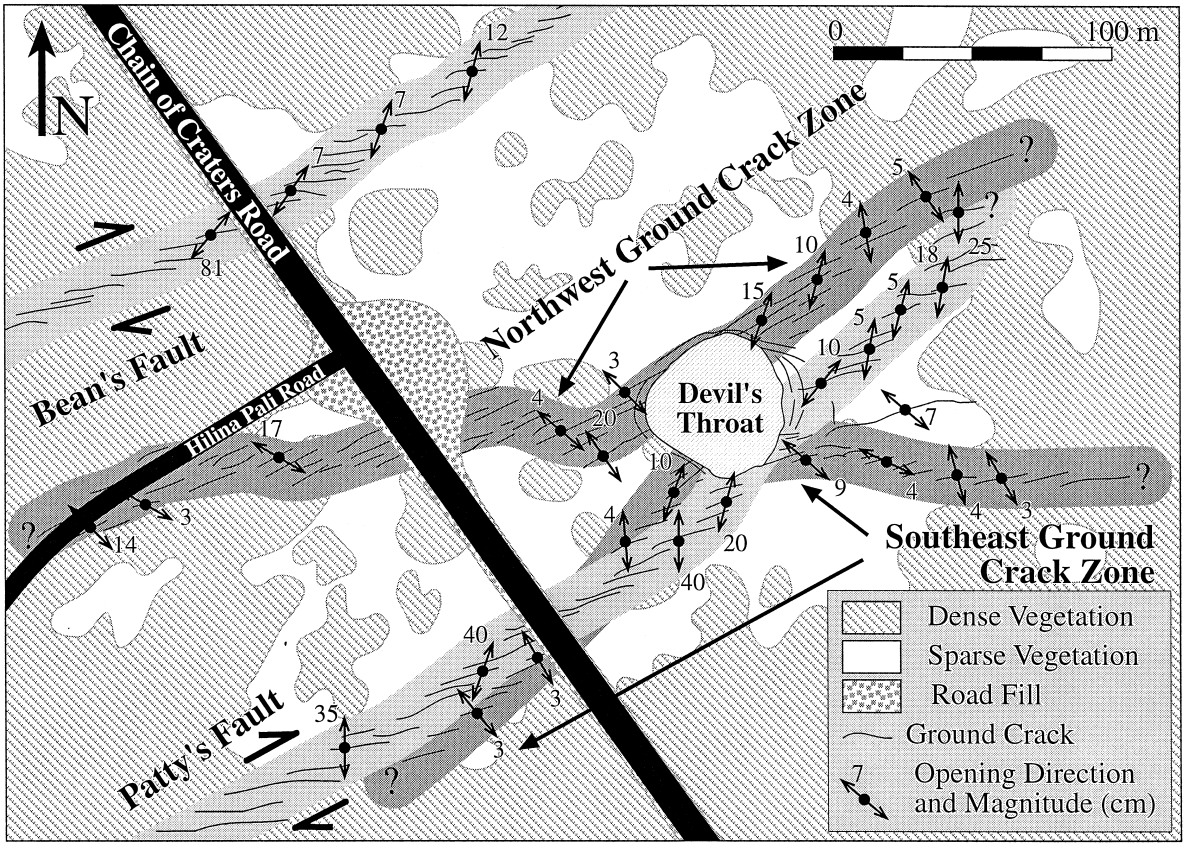

Fig. 3. Structural map of Devil's Throat pit crater showing the Northwest and Southeast Ground Crack Zones, and Bean's and Patty's Faults. Devil's Throat lies at a waist between the Northwest and Southeast Ground Crack Zones.

of Patty's fault extends approximately 1 km west of Devil's Throat. Individual fractures along Patty's Fault generally have an average dilation direction perpendicular to their strike. The individual fractures also step to the left and generally have trace lengths slightly greater than those of Bean's fault. Both faults are currently active and disrupt Chain of Craters Road, with Patty's Fault being the more active of the two.

Zones of cracks intersect the northwest and southeast walls of Devil's Throat; we refer to these as the Northwest and Southeast Ground Crack Zones, respectively (Fig. 3). The cracks can be located readily owing to the ferns that grow out of them. The latter zone intersects Patty's Fault 150 m west of Devil's Throat and again at the pit's southeast rim. At distances greater than 40 m from the present-day crater rim, the surface traces of the two crack zones have an average strike of N 60° E and are more than 50 m apart. Closer to the pit, the traces of the crack zones converge toward each other and form an 'hourglass' pattern. At the rim of the pit, the traces of the two crack zones are approximately 25 m apart.

Individual cracks within the zones are en echelon where the crack zones converge near the pit rim. Individual cracks have an average strike of northeast and an average northwest–southeast dilation direction; dilation directions were determined by matching originally neighboring points on opposing walls of a fracture. The local dilation direction of cracks in these zones is roughly at right angles to the overall strike of the crack zones.

Cracks within these zones extend down the height of the pit wall. The cracks of each crack zone dip toward the opposite crack zone at angles greater than 87°. Fractures in the northeast and southwest walls of

the pit are much more prominent than fractures in the northwest or southeast walls, indicating that the most prominent subsurface fractures at Devil's Throat strike roughly northeast.

3. Pit craters of the Southwest Rift Zone of Kilauea

A series of pit craters is also exposed along the Southwest Rift Zone (SWRZ) of Kilauea, most astride the Great Crack (Fig. 1a). The SWRZ can be divided into two main segments, the Upper SWRZ, which extends 15 km downrift from Kilauea caldera, and the Lower SWRZ, which extends the remaining 20 km to the coast. The Upper SWRZ strikes southwest and the Lower SWRZ strikes south-southwest. The Upper SWRZ contains two distinct parallel zones of ground cracking, the northern and southern arms of the Upper SWRZ, which are spaced 1–2 km apart (Fig. 1). The Great Crack is located within the Lower SWRZ and is expressed as a linear series of ground cracks, grabens, pit crater chains, and chasms. The fractures along the Great Crack dip steeply, and locally the walls of the grabens overhang. Volcanic features of the SWRZ are similar to those of the ERZ, although less historic eruptive activity has occurred on the SWRZ. The SWRZ is located, for the most part, within the Ka'u Desert, and dense vegetation is limited to scattered kipukas.

Ground cracks are well exposed in the SWRZ owing to its location within the Ka'u Desert. The rift zone ground cracks nearly parallel the rift zone axis. Additionally, faults concentric about Kilauea caldera intersect the northern and southern arms of the Upper SWRZ. The Southern arm of the Upper SWRZ intersects the western end of the Koa'e Fault Zone (Fig. 1). At their intersection, the ground cracks of the Koa'e Fault Zone are sub-parallel with the ground cracks of the southern arm of the SWRZ.

The pit craters along the SWRZ are about as numerous as those of the East Rift (Fig. 1), but references to them have not been found in the scientific literature. The Twin Craters are located on the southern arm of the Upper SWRZ, and Wood Valley pit crater is located on the northern arm of the Upper SWRZ. We have identified fourteen pit craters along the Lower SWRZ, along the northern end of the Great Crack. These are either single, occur in chains, or have coalesced. Some pit crater chains have coalesced into 'pit troughs' with scalloped sides.

The pit craters of the Southwest Rift Zone are well exposed owing to a lack of dense vegetation, but are infrequently visited owing to their remote location within the Ka'u Desert. These pit craters are generally smaller in depth and diameter than the majority of the ERZ pit craters. Some pit craters are, however, roughly equal in size to Devil's Throat and Lua Nii. Similar to Devil's Throat and Lua Nii, many of the SWRZ pit craters are known to contain caves at their bases. The SWRZ pit craters are not intersected by fissure vents, and they contain no ponded lava from near-by vents. These pit craters lack radial flows and are not ringed by phreatic ejecta, indicating that they did not originate as vents for effusive or explosive eruptions. None of the pits contain an apparent floor of ponded lava, but instead are floored by talus.

3.1. Pit craters of the Upper Southwest Rift Zone

Three upper SWRZ pit craters have been explored by cavers. Favre (1993) explored the eastern Twin Crater (Fig. 1c). He found a cave of undetermined length at the western base of the pit. A smaller cleft in the eastern base of the pit is indicated in his cross-section of the pit. Favre also noted that the lower 15 m of the pit walls were coated with a chilled margin of lava. Whitfield (1980) explored the western Twin Crater (Fig. 1c). Whitfield did not indicate the absence or presence of caves at the base of the pit, but noted that a connection to the eastern Twin Crater, approximately 40 m to the east, could not be found. Favre (1993) also explored Wood Valley pit crater (Fig. 1b), which is located along a fracture that extends a few kilometers to the northeast to Ponohohoa Chasms, as well as several hundred meters to the southwest of the pit. This fracture is parallel with the local strike of the SWRZ. Through an opening in the talus at the base of the pit, Favre discovered an extensive linear cave with an average height of 8 m, average width of 5 m, and a length of greater than 460 m, at a depth of 90 m. The walls of the cave were coated with chilled lava. Favre encountered two large chambers along the length of the cave. The first was located directly below the pit and

was nearly filled by the talus that serves as the pit floor. Further along the cave, the second chamber is completely intact, and measures 40 m high, 10 m wide, and 40 m long. Favre noted numerous fractures visible in the chamber ceiling and walls striking parallel to the long axis of the chamber. We visited Wood Valley pit crater and observed prominent, near-vertical fractures in the northeast and southwest walls of the pit. These fractures cannot be traced on the surface, which consists of 'a' a clinker and loose volcanic ash.

3.2. Present-day observations of the Great Crack pit craters

A series of little-known pit craters also exist astride the Great Crack (Fig. 1a), a 15-km-long fracture system along the Lower SWRZ. We have identified fourteen pit craters along the Great Crack (Table 1). These pits range in diameter from 8 to 45 m and in depth from 6 to 28.5 m. Lava flows exposed in the walls of the pit craters generally range in thickness from about half a meter to several meters. The blocks of talus mantling the floor and walls of the pits also typically have linear dimensions of half a meter to several meters, with most being 1–2 m long. The larger blocks appear to be derived from the thicker flows. The pits are located along depressions that locally contain near-vertical ground cracks that are at least several meters deep and that have apertures of several centimeters. Pits A through E are centered on a continuous depression 5–7 m wide and 2–15 m deep. This depression locally is filled with talus and volcanic ash. Pits F through N are centered on a shallower depression that generally is 10–15 m wide and 0.5–2 m deep. This depression locally contains steep-walled troughs 5–7 m wide and 2–3 m deep. Where this depression intersects the northeast and southwest walls of Pit F, it is filled with volcanic ash, whereas the ground cracks and fractures at pits G through N, as well as the pits themselves, do not contain visible accumulations of ash. Near-vertical fractures are prominent in the northeast and southwest walls of the pits, where the Great Crack intersect the pits.

Many of these pits contain caves and overhangs at the bases of their northeast and southwest walls, where the Great Crack intersects the pit walls. We observed all but a few of these caves from the pit crater rims but did not explore them. The visible portion of the cave entrances typically attain heights and widths of a few meters. The largest cave was observed in the southwest wall of Pit H. This cave is estimated to be 10 m wide and 15 m tall. The top of the cave rises to the base of Pit H's talus floor and appears to extend at least 30 m beyond the pit wall to the southwest.

Pit H has formed recently. It is now one of the largest SWRZ pit craters, but it does not appear on a 1:6000 scale, 1965 aerial photograph of the Great Crack. Neighboring pit G, which is smaller than pit H, is clearly visible on the 1965 photograph. The photograph shows Pit G between a pair of parallel fractures spaced about 5 m apart. A talus-filled depression extended approximately 25 m downrift from Pit G along the Great Crack. This former trough is now the site of Pit H. A 5 m wide, 2 m deep talus-filled depression now extends southwest of Pit H.

Several pits have coalesced. Pits G and H share a fragile 1 m wide, 2 m tall septum, the top of which is approximately at the same elevation as the surrounding ground surface. Talus that slopes into the pit bottoms flanks the septum. In map view, these two pits have a 'figure 8' outline. Likewise, Pits J and K have coalesced and are separated by low septa, which are nearly covered by talus. The coalesced pits L, M, and N are nearly circular, with similar diameters and depths, and are separated by septa 2–3 m tall.

Downrift of Pit N, a continuous series of 'pit troughs' extends along the Great Crack. The pit troughs are scalloped-sided with local septa-like ridges extending from the walls into the center of the rough. The pit troughs are roughly 30–40 m wide and 15–20 m deep. Cave entrances and overhangs are visible in the northeast and southwest ends of some of these pit troughs, at the intersection of the Great Crack. The pit troughs extend 2 km along the Great Crack and lead into a continuous, steep walled depression, 6–10 m wide and 12–15 m deep. This steep-walled depression extends 8 km downrift along the Great Crack. The pit troughs and adjoining steep walled depression form a 10-km-long depression along the Great Crack. The 1823 Keaiwa flow

(Stearns, 1926; Stone, 1926) welled up along the length of this section of the Great Crack.

4. Observations at Kilauea from 1919–1922

Jaggar (1947) described some spectacular fissuring and stoping in the southwest wall of Kilauea caldera between 1919 and 1922. In November 1919, a fracture, termed Red Solfatara, appeared in the southwest wall of Halema'uma'u pit, within Kilauea caldera. The fracture extended approximately 120 m up from the pit floor but did not reach the surface outside the pit. The aperture of this fracture increased with depth. On December 15, 1919, ponded lava from Halema'uma'u began flowing into this fracture, and fissure vents opened up on the southwest rim of Kilauea Caldera where intersected by the SWRZ. This fracture piped lava from Halema'uma'u, and the eruption ceased as soon as the elevation of the lava lake in Halema'uma'u dropped to the elevation of the vents (Jaggar, 1947). One of the fissures outside Halema'uma'u had a surface aperture of 1.5 m, a measured depth of 24 m, and began emitting gases at a temperature greater than 40°C. Six days later this fissure had opened to nearly 4.5 m, and lava could be observed flowing in it about 15 m below the surface. By March of 1921, 'impressive underground chambers' that served as a 'flow tunnel' were observed along the Red Solfatara fracture. Later that autumn, Jaggar describes the Red Solfatara fractures as 'an open vaulted rift chasm' and lava was observed flowing along it. The description of May 26 is particularly revealing: ''The huge cavern of the 1920 rift... gashing the southwestern inner wall of Halema'uma'u vertically, became a black tunnel half as high as the pit wall, with a lava pool inside the tunnel and incandescent rock falling from its ceiling.'' The pit wall at the time was estimated to be 200–250 m tall. Based on these descriptions and an accompanying photograph, the void Jaggar described appears to have been at least 100 m tall and 20 m wide. Within two days, ''The tunnel... fell in, making a smoking canyon that extended as a bay in the Halema'uma'u rim 500 ft [150 m] in that direction... The new pit was therefore a pointed oval in plan, with the point directed toward the Ka'u desert.'' These descriptions are of stoping into a progressively widened subsurface fracture.

5. Conceptual model

An explanation for pit crater formation must account for the following characteristics:

1. The location of pit craters along rift zones;
2. The abundance of steep fractures in the pit walls;
3. Pairs of ground crack zones near pit crater margins;
4. The elliptical geometry of pit craters in map view;
5. Steep, overhanging pit crater walls;
6. The presence of caves along the long axis of many pit craters.

In addition to these characteristics, a valid model must also be consistent with the observations of Jaggar (1947) from 1919–1922. Because of the predominance of opening-mode displacements across fractures near the pit craters, we do not consider strike-slip faults to be a central characteristic of pit craters.

We suggest that a pit crater forms in response to stoping into a tall, steep, subterranean opening-mode rift zone fracture with an uneven upper edge (Fig. 4). As this fracture opens and propagates upward, a pair of ground crack zones forms at the surface. We do not expect the top edge of the fracture to be straight and parallel to the surface owing to variations in the resistance to fracturing of the host rock. For example, where the fracture encounters a pre-existing weakness, such as a fault or a sequence of thin lava

Fig. 4. Proposed fracture-induced origin of Kilauea's pit craters. (a–c) An opening-mode fracture propagates under some combination of fluid pressure or far-field tensile stress. The top of the fracture may form a cusp in an area of preexisting structural or stratigraphic weakness in the host rock (i.e., faults, thin lava flows). (d) The roof of the fracture caves in. Enhanced collapse may occur where the fracture encountered a preexisting structural or stratigraphic weakness. Magma flow through the fracture may aid the stoping process by evacuating debris. (e) The void breaches the surface and forms a pit crater. Initially, the pit crater has a small aperture surface opening leading into a cupola-shaped void. The pit grows by further roof and wall collapse.

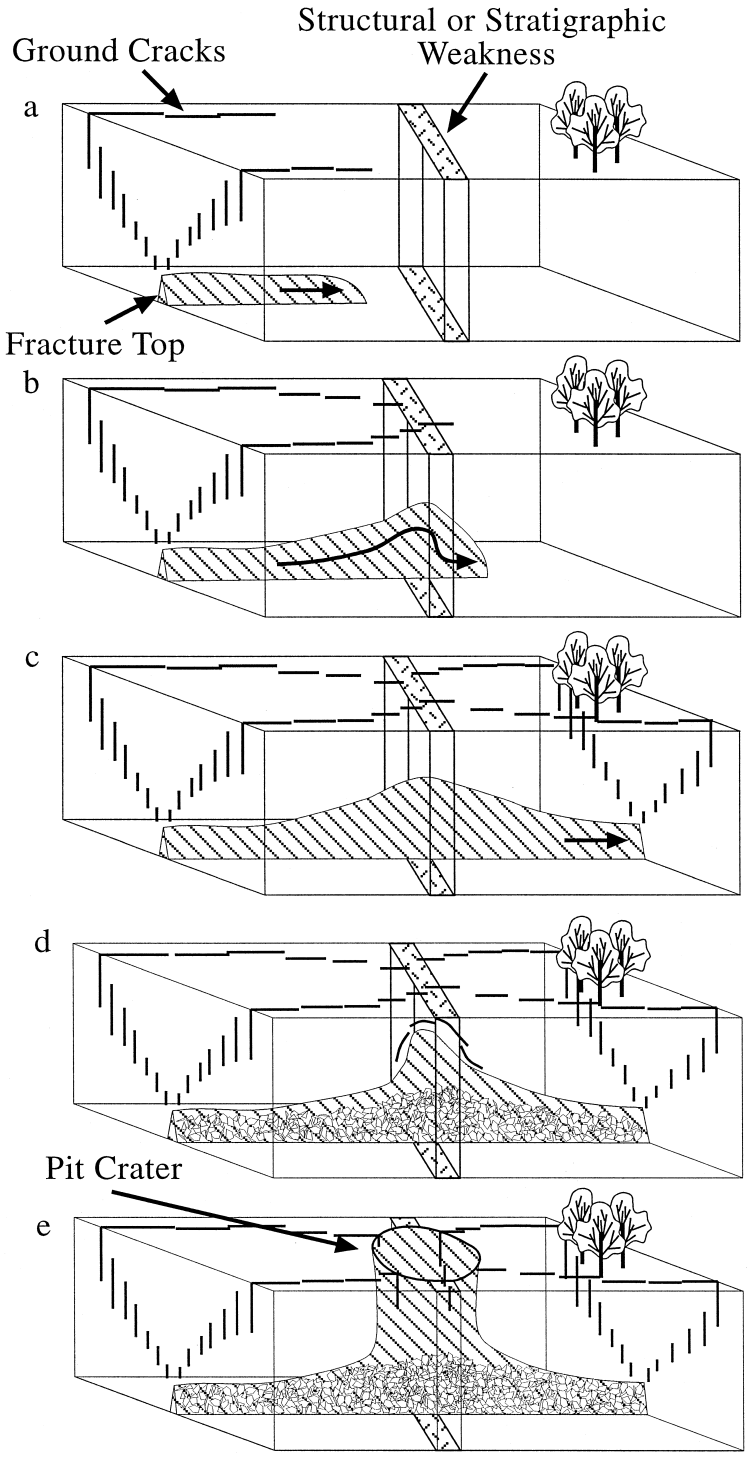
Structural or Stratigraphic Weakness
Ground Cracks
a
Fracture Top
b
c
d
Pit Crater
e

flows, its local vertical propagation rate can increase, resulting in a fracture with an uneven upper edge. Stoping of the already-fractured volcanic host rock adjacent to and above the fracture creates an upward-migrating, cupola-shaped collapse chimney. Continued stoping eventually leads to collapse at the surface and a pit crater is formed. Some of the surface collapse will be localized along the ground crack zones at the surface, leading to elliptical-shaped pit craters.

For this process to be viable, the fracture must have an aperture larger than the blocks being stoped. Stoping above a typical Hawaiian dike seems implausible owing to the small dike apertures. For example, a dike intruded along the Kilauea's SWRZ in 1981 has been inferred to have an average thickness of only slightly more than 1 m based on geodetic data (Pollard et al., 1983). Most dikes observed in the Hawaiian islands are, on average, less than a meter thick (Walker, 1987). Dikes this narrow could not admit the 1–2-m-long talus blocks seen in the pit craters. Larger aperture fractures might be opened along Kilauea's rift zones by a combination of magma pressure and tensile stresses associated with the seaward sliding of the Kilauea's south flank. As an example, horizontal surface displacements associated with the 1975 Kalapana earthquake reached 8 m (Lipman et al., 1985). If this amount of displacement were accommodated across a single fracture, it could readily accept meter-scale stope blocks. Magma flow through a large-aperture fracture could assist the stoping process. Magma flow could evacuate stope blocks as well as widen the fracture through thermal and mechanical erosion of its walls. A combination of these processes may account for the 4.5-m-aperture fissure described by Jaggar (1947) and the dimensions of the openings described by Favre (1993) beneath the Wood Valley pit crater.

Our proposed model is consistent with the six listed pit crater characteristics, as well as with the 1919–1922 observations of Jaggar (1947). The rift zones are where the south flank of Kilauea is separating from the north flank and are the centers of magma intrusion (Duffield, 1975; Denlinger and Okubo, 1995). Both south flank displacement and magma intrusion play important roles in generating and maintaining a large-aperture fracture into which stoping may occur. As we will discuss in the next section, the abundance of steep fractures in the pit walls, as well as the pairs of ground crack zones near pit crater margins, arise as a consequence of tensile stresses concentrations above an opening-mode fracture. The elliptical geometry of the pit craters is consistent with collapse along the paired ground crack zones, or above the open fracture itself. As shown by the observations of Jaggar (1947), stoping naturally leads to a cupola-shaped collapse chimney and can account for steep or overhanging pit crater walls. Finally, the presence of caves along the long axis of the pits is consistent with stoping into a vertical rift fracture that extends beneath and beyond the pits.

6. Mechanical analyses

Although geometric arguments support stoping into a vertical fracture as a possible mechanism for pit crater formation, other considerations dictate an examination of the mechanics of opening-mode fractures. We start by examining fracturing as seen in map-view and in cross-section, and then consider the pattern of ground cracks observed at Devil's Throat.

Two characteristics of pit craters listed in the previous section are (1) pairs of ground crack zones at the margins of the pit craters and (2) an abundance of steep fractures in the pit walls. The fractures observed within the ground crack zones and within the pit walls are predominantly of opening mode. This is consistent with our conceptual model. As shown in Fig. 5, tensile stresses are concentrated above the tip of an opening-mode fracture (Lawn and Wilshaw, 1975). Furthermore, the maximum tensile stresses form two distinct lobes on either side of the fracture (Pollard et al., 1983; Pollard and Segall, 1987). These lobes form a 'V' pattern, with the vertex of the 'V' being closest to the top of the opening-mode fracture. In these lobes of concentrated tensile stress, the predicted trajectories normal to the most tensile stress are steep. A similar pattern occurs above a pressurized dike (Pollard et al., 1983). The patterns are similar because two effects common to both scenarios dominate the stress field above the fracture: (1) the near-tip stress field associated with the opening-mode fracture; and (2) the influence of the stress-free ground surface. Owing to the domi-

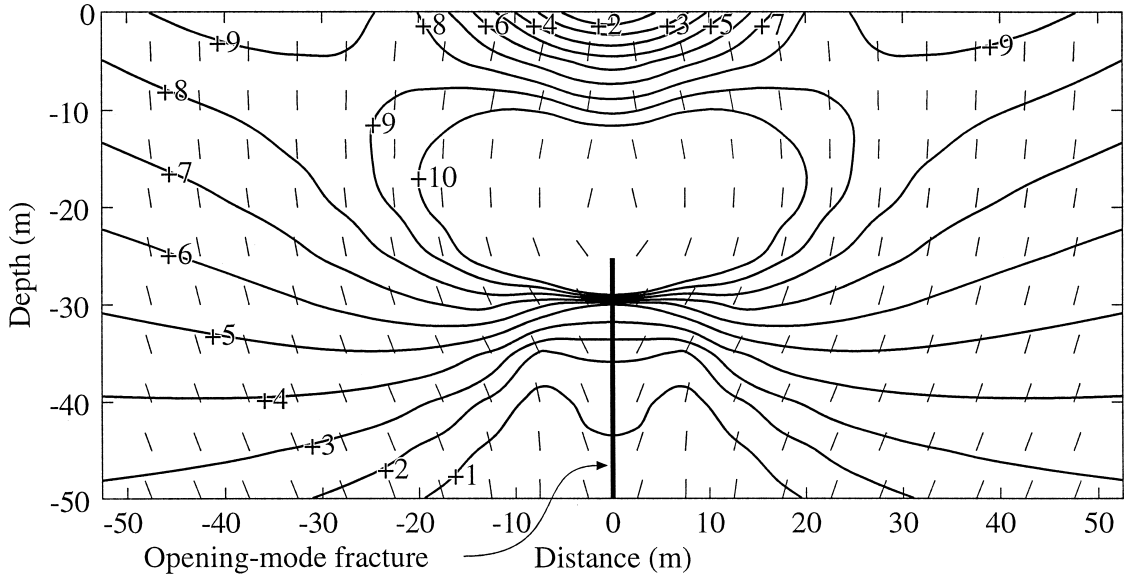

Fig. 5. Contours of the most tensile stress near the top of a vertical opening-mode fracture. The ambient vertical stress is ρgy, where $\rho = 2700\ \mathrm{kg/m^3}$ and the horizontal far-field stress is 1 MPa. The crack is stress free and extends from -1025 m to -25 m. The short ticks are trajectories perpendicular to the most tensile stress and represent the orientations of potential ground cracks. Ground cracks are predicted to open within the two lobes of concentrated tensile stress above and on either side of the fracture tip. The character of the stress field is very similar to that over the pressurized dike modeled by Pollard et al. (1983) even though the geometry and boundary conditions are rather different.

nance of these effects, the stress field above the tip of an opening-mode fracture subject to a broad range of far-field stresses and fracture pressures will resemble that of Fig. 5. New cracks that open above the fracture would be oriented perpendicular to the trajectories of the most tensile stress and therefore dip steeply. Pre-existing vertical cracks, such as thermal contraction cracks in lava flows, also would open. Fig. 6 illustrates the resulting pattern of ground cracks in map-view and in cross-section above a deep (a), intermediate (b), and shallow (c) opening-mode fracture. As seen in map view, these cracks would strike parallel to the underlying opening-mode fracture. They also would tend to cluster in a pair of crack zones, one on either side of the fracture. In cross-section, the cracks will be clustered within the two lobes of concentrated tensile stress and therefore form a 'V' pattern. The spacing between the pair of crack zones will tend to scale with the depth to the top of the opening-mode fracture. As a result, crack zones at the surface will tend to converge where the depth to the top of the opening-mode fracture decreases. Above very shallow fracture tops, separate ground crack zones might be indistinguishable. This pattern of ground cracks has been described for dikes by several investigators (e.g., Fink and Pollard, 1983;

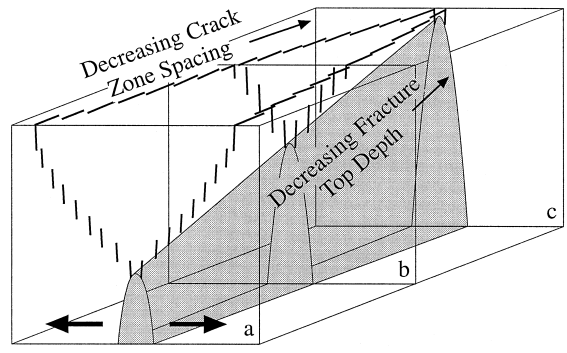

Fig. 6. Schematic diagram of the pattern of ground cracking (short ticks) above a deep (a), intermediate (b), and shallow (c) opening-mode fracture top. Note that in cross-section, the 'V' pattern of ground cracks arises from two lobes of concentrated tensile stress on opposing sides of the fracture (see Fig. 5). A deep fracture top is expected to generate a widely-spaced pair of ground crack zones, whereas shallower fracture top depths are expected to yield closely-spaced ground crack zones.

Pollard et al., 1983; Mastin and Pollard, 1988). These fractures would become exposed in the walls of a pit as stoping above the subsurface fracture extends to the surface. Therefore, the concentration of tensile stress above the tip of a subsurface opening-mode fracture can account for the observed abundance of steep tensile fractures within and around the pit craters, as well as pairs of ground crack zones at the margins of the pit craters.

As previously mentioned, a particularly interesting pair of ground crack zones exists at Devil's Throat pit crater; the pair of ground crack zones have an 'hourglass' pattern. To test the possibility that this 'hourglass' fracture pattern around Devil's Throat reflects tensile stress concentrations above a subsurface opening-mode fracture with an irregular top underlying the pit, we applied a three-dimensional fracture modeling code, POLY3D (Thomas, 1994). This code is based on the boundary element method (e.g., Crouch and Starfield, 1983; Schultz and Aydin, 1990). The technique works by dividing the walls of the fracture into a series of polygonal elements (Fig. 7), and then determining the relative displacement distribution of the fracture wall elements necessary to yield the desired boundary conditions on the fracture walls (Martel and Boger, in press).

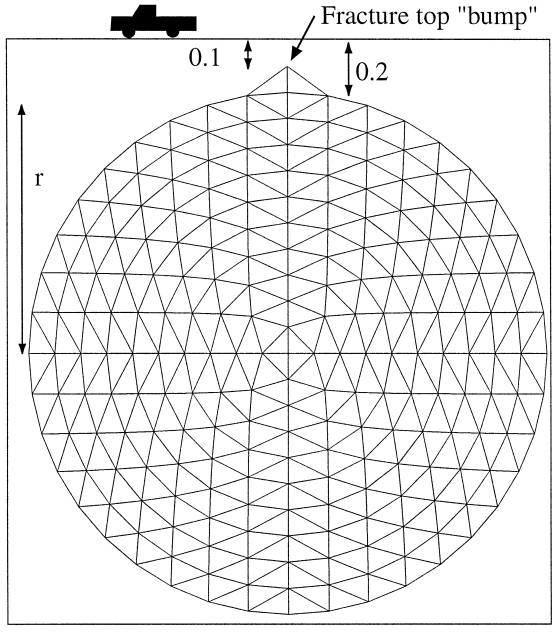

Fig. 7. Three-dimensional boundary element model of a fracture with an irregular top showing the distribution of elements.

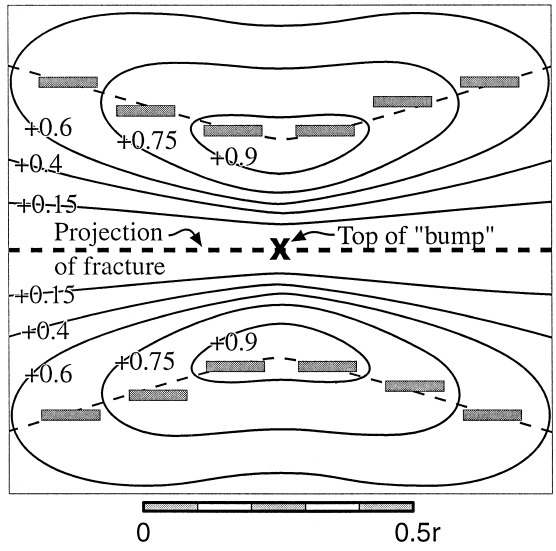

Fig. 8. Magnitude of the most tensile stress at the surface (contours) and trajectories normal to the most tensile stress (bars) above the opening-mode fracture of Fig. 7. The stress magnitudes are normalized by the unit driving stress. Ground cracks are predicted to form along the dashed lines with an orientation parallel with the bars. This plot suggests that a subsurface fracture could have produced a pair of converging crack zones as seen at Devil's Throat and at other pit craters.

We modeled a vertical, nearly circular opening-mode fracture with a small bump on its top. Here the boundary condition was a uniform unit driving stress. The depths from the surface to the top and to the base of the bump were set to one-twentieth and one-tenth the fracture height, respectively. Strains, stresses, and displacements were then calculated from the displacements of the polygonal wall elements. Fig. 8 shows the resulting contour plot of the magnitude of the most tensile stress *perturbation* on the ground surface due to opening of the fracture. These stresses are scaled relative to the driving stress for the fracture. The projection of the fracture to the surface is shown by a heavy dashed line, and an 'x' is above the top of the fracture. Note that the closed contours are shaped like bent ovals; a pair of light dashed lines marks the axes of these closed contours and show where ground cracks would be expected. These lines form an hourglass pattern. The 'waist'

between the lines occurs abreast the top of the fracture. The distance between the lines at the waist is about half that near the edge of the plot. The heavy bars along the dashed lines are oriented perpendicular to the most tensile stress at the surface and essentially parallel the strike of the model fracture. The orientation of these bars gives the expected orientation of ground cracks. This geometry resembles that of the Northwest and Southeast Crack Zones at Devil's Throat (Fig. 3). This same pattern would be produced if a near-surface fracture were either pulled open or pushed open by fluid pressure. An opening-mode fracture widened by stoping would also yield a similar stress perturbation.

Although the fracture geometry at Devil's Throat could be substantially different from that of Fig. 7, a comparison of Figs. 3 and 8 show that the position and orientation of the observed fractures in the Northwest and Southeast Crack Zones at Devil's Throat are consistent with an opening-mode fracture that approached the surface most closely beneath the pit crater. The paired ground crack zones observed at Devil's Throat and at other pit craters could have formed above, and as a result of, an opening-mode fracture propagating towards the surface.

7. Discussion

The mechanism we propose fits a variety of observations and is mechanically viable. Before discussing implications of our model, however, we first re-examine other proposed mechanisms for pit crater formation.

Stearns and Clark (1930) suggested that pit crater formation begins through stoping above a magma-filled fracture, and that after subsidence of the magma, roof collapse occurs in the area of stoping and leads to the formation of a pit crater. Their model resembles ours, except that we do not see the need for the fracture to be filled with magma and admit the possibility that regional tensile stresses could open the fracture. We acknowledge that changes in the level of magma in a fracture could cause stress changes along its walls that contribute to stoping, especially after some stoping has already occurred. Under those conditions, decreases in magma level cannot lead to full closure of the fracture.

Favre (1993) suggested that some pit craters may form above partially drained dikes. This too is similar to our model but, as noted previously, normal dikes have too small an aperture to provide a viable means for stoping. Significantly, Favre's description of chilled lava on only the lower part of one chamber beneath Wood Valley pit crater indicates that subsurface fractures need not be filled with magma to generate pit craters.

Walker (1988) proposed that pit craters form due to stoping over a deep, long-lived, active conduit that transports magma from the Kilauea summit chamber into the rift zone. This is compatible with our model; indeed the overall geometry of Walker's proposed collapse chimney resembles a tall fracture in cross-section. Walker envisions a magma conduit at the base of the collapse chimney that is subhorizontal and cylindrical. We do not see the need for a conduit of this geometry, however, and invoke a different conduit geometry that is more compatible with the descriptions of Jaggar (1947).

The hypothesis by Blevins (1981) that pit craters on Kilauea are the result of roof collapse over a broad cavity with an aerial extent of several square kilometers seems untenable. This mechanism does not account for the location of the pit craters along a narrow belt or the presence of narrow graben-like depressions that extend into the pit craters. It predicts broad subsidence bowls along the rifts which are not observed. We also do not see a way to support a roof of fractured volcanic rock over such a broad cavity.

Piston-like ground subsidence over a large, depressurized, near surface magma reservoir (e.g., Macdonald et al., 1990; Hirn et al., 1991; Senske et al., 1992) does not seems to be a viable mechanism for pit crater formation. This mechanism does not account for the overhanging walls, the presence of the pit crater caves, the associated graben-like depressions, or the abundance of fractures in the pit crater walls.

One implication of our model of pit crater formation is that the caves observed at the base of pit walls may in fact mark the top of stoping below and beyond the area of the pits. To examine this possibility we return to the pairs of ground cracks at the surface.

Fink and Pollard (1983) and Pollard et al. (1983) suggest that the distance between the innermost cracks of the paired ground crack zones above a dike of finite height is approximately 2–3 times the depth of the dike top. Experiments in granular materials by Mastin and Pollard (1988) subsequently showed that this crack zone spacing gives a minimum depth to the dike top owing to inelastic deformation above the dike. They suggested that the distance between the outermost cracks of the paired ground crack zones is a better indicator of dike top depth. Their experimental results show the ratio of the spacing between outermost cracks to the depth of the dike top ranges from 0.5 to 2. Variations in this depth-to-spacing ratio were attributed to differences in the shape of the dike top and differences in the degree of inelastic deformation above the dike.

If the caves at the base of the pit walls represent the top of a fracture modified by stoping, then the ratio of the pit crater short axis to the pit crater depth should serve as a proxy for the ratio of the ground crack zone spacing to fracture depth. Our observations show that the spacing between ground crack zones, or the width of the grabens leading to the pit craters, is close to the short dimension of the pit crater. The depth of the pits is likewise similar to the depth to the top of the caves, for the caves typically extend only a few meters above the talus on the pit crater floors. An inspection of Table 1 shows that the ratio of the pit crater short axis to the pit crater depth is between 0.5 and 2 for every pit with an observable cave except for pit N, where the ratio is 2.6. This is an excellent match with the experimental results of Mastin and Pollard (1988) and supports our hypothesis that stoping is occurring into a steep fracture that extends nearly to the surface.

We suggest that magma flow through a subterranean open fracture could help the stoping process by evacuating debris which could otherwise choke the fracture and arrest the stoping process. We will now consider this process in greater detail.

Although a large-aperture fracture need not be filled with magma, observations reported by Jaggar (1947) on the 1919–1922 eruption of Kilauea reveal that large-aperture fissures along the SWRZ did contain magma. Flowing magma provides a means for debris removal and hence helps sustain stoping. Stoping was observed along the southwest wall of Halema'uma'u, but stope debris has not been recognized within the products of effusive eruptions—why?

A simple explanation is that the debris fell to the bottom of the fracture. Stoped debris is unlikely to be erupted if it is lodged there. The feasibility of this explanation can be assessed by determining the settling speed of stope debris through basaltic magma. Settling speeds of blocks must be sufficiently high such that stoped blocks settle to great depth before they can be erupted downrift.

The equilibrium speed of a mass falling through magma can be approximated by equating the resisting shear force of magma and the driving force of gravity on the mass. Assuming a Newtonian rheology for the magma:

$$(1/2\,\rho_0 v 2)\,AC_D = (\rho_1 - \rho_0)Vg \qquad (1)$$

where v is the fall speed, ρ_1 the density of rock, ρ_0 the density of magma, A the frontal area of the mass, C_D a dimensionless drag coefficient, V the block volume, and g the acceleration of gravity. Solving for the fall speed v yields:

$$v = \left[(2(\rho_1 - \rho_0)Vg)/(\rho_0 AC_D)\right]^{1/2} \qquad (2)$$

We consider blocks with a linear dimension of 1.25 m. This dimension is consistent with our observations of talus blocks in pit craters. To estimate fall speed, we use a rock density (ρ_1) of 2730 kg/m^3, a magma density (ρ_0) of 2600 kg/m^3, and a magma viscosity of 50 Pa/s. The dimensionless drag coefficient C_D depends on block shape. To determine the drag coefficient (C_D) of the falling mass, we approximate its shape to be a sphere, for which Lapple (1950) plotted C_D vs. Reynolds number. An initial estimate for fall speed is required to calculate the Reynolds number, which in turn is used to calculate a final fall speed using Eq. (2). This process can be repeated recursively and converges to a fall speed of 0.64 m/s.

These calculations show that stoped debris can fall through several hundred meters of magma within a few hours. Unless an eruptive vent were located within several hundred meters of where stoping occurred, this time should be sufficient to preclude the eruption of a stope block. Additionally, the debris may simply become stuck in narrow sections of a fracture. These two mechanisms enable stoped debris

to be retained within a fracture, preventing its eruption.

No pit craters have been identified along the Koa'e fault zone (Fig. 1), and our proposed mechanism might shed light on their absence. The Koa'e fault 'zone' is actually a region of distributed normal faulting that is bounded on the east by the Upper ERZ and on the west by the Southwest Rift Zone (Duffield, 1975; Swanson et al., 1976). Dike intrusion into the Middle and Lower ERZ is considered to contribute significantly to driving displacement of the south flank of Kilauea (Duffield, 1975; Swanson et al., 1976). Dike intrusion directly into the Koa'e region, however, is infrequent (Duffield, 1975; Holcomb, 1987). The apparent absence of pit craters along the Koa'e faults might be due to three reasons. First, the low level of magma intrusion might be inadequate to help flush stope debris from the fractures. Second, owing to the number of fractures, the amount of opening accommodated by individual fractures might be small, too small to allow stoping to proceed freely. Third, if magma were absent, then the available driving pressure might be too low to help open a large-aperture fracture.

East Rift pit craters are substantially larger than those along the SWRZ (see Table 1). Our mechanism for pit crater formation provides a possible reason why. Geodetic surveys show that surface displacements on the south flank of Kilauea are primarily directed to the southeast (e.g., Denlinger and Okubo, 1995). This is nearly perpendicular to the ground cracks of the Upper East Rift, but at an acute angle to those of the Southwest Rift. As a result, fractures of the East Rift are likely to open more than those on the Southwest Rift. This would lead to larger pits on the East Rift, consistent with experimental results of Mastin and Pollard (1988).

8. Conclusions

Stoping into a nearly vertical subsurface opening-mode fracture provides a viable mechanism for the formation of pit craters along the East Rift and Southwest Rift of Kilauea volcano. This process accounts for the common attributes of pit craters: (1) their location along rift zones; (2) the abundance of steep fractures in the pit walls; (3) pairs of ground crack zones near pit crater margins; (4) the elliptical geometry of pit craters in map view; (5) steep, overhanging pit crater walls; and (6) caves along the long axis of many pit craters. The ratio of pit crater width to depth of 0.5 to 2 is also consistent with pit craters forming over a nearly vertical opening mode fracture. A combination of magma intrusion and seaward migration of Kilauea's south flank provides a means of generating such fractures. Magma flowing through the fracture would help the stoping process.

Acknowledgements

Comments by Stephen Self, Larry Mastin, Elisabeth Parfitt, and Lionel Wilson contributed to substantial improvements in the manuscript. Scott Rowland provided helpful insight into Hawaiian volcanoes. William Halliday shared valuable information on pit craters and vulcanospeleology. Discussions with David Bercovici and Amanda Kelly regarding magma dynamics are gratefully acknowledged. We thank Bill Boger for running our POLY3D models. Mr. Ken Fujiyama graciously granted us access to many of the Southwest Rift Zone pit craters. Many thanks to our faithful field assistants Charles Budney, Chris Peterson, and Greg Smith. This work was supported by grants from the Office of Naval Research (N00014-96-1-0353), the US Department of Energy (DE-FG03-95ER14525), and the Department of Geology and Geophysics, University of Hawaii at Manoa. This is HIGP paper No. 993 and SOEST contribution No. 4635.

References

Blevins, J.Y., 1981. Subsidence mechanics of Kilauean pit craters. M.S. thesis, University of Hawaii.

Carr, M.H., Greeley, R., Blasius, K.R., Guest, J.E., Murray, J.B., 1977. Some martian volcanic features as viewed from the Viking Orbiters. J. Geophys. Res. 82, 3985–4015.

Crouch, S.L., Starfield, A.M., 1983. Boundary Element Methods in Solid Mechanics. Allen and Unwin, London.

Denlinger, R.P., Okubo, P., 1995. Structure of the mobile south flank of Kilauea volcano, Hawaii. J. Geophys. Res. 100, 24499–24507.

Duffield, W.A., 1975. Structure and origin of the Koae Fault System, Kilauea volcano, Hawaii. US Geol. Surv. Prof. Pap. 856.

Favre, G., 1993. Some observations on Hawaiian pit craters and relations with lava tubes. In: Halliday, W. (Ed.), Proceedings of the 3rd International Symposium on Vulcanospeleology. International Speleological Foundation, Seattle, WA, pp. 37–41.

Fink, J.H., Pollard, D.D., 1983. Structural evidence for dikes beneath silicic domes, Medicine Lake Highland volcano, California. Geology 11, 458–461.

Halliday, W.R., in press. Pit craters, lava tubes, and open vertical volcanic conduits in Hawaii: a problem in terminology. In: Proceedings of the 8th International Symposium on Vulcanospeleology. National Speleological Society, Huntsville, AL.

Hirn, A., Lepine, J., Sapin, M., Delorme, H., 1991. Episodes of pit-crater collapse documented by seismology at Piton de la Fortunaise. J. Volcanol. Geotherm. Res. 49, 89–104.

Holcomb, R.T., 1976. Preliminary map showing products of eruptions, 1962–1974 from the upper east rift zone of Kilauea volcano, Hawaii. US Geol. Surv. Misc. Field Studies Map, MF-811.

Holcomb, R.T., 1987. Eruptive history and long term behavior of Kilauea volcano. In: R.T. Decker, T.L. Wright, P.H. Stauffer (Eds.), Volcanism in Hawaii. US Geol. Surv. Prof. Pap. 1350, 261–351.

Jaggar, T.A., 1912. Report of the Hawaiian Volcano Observatory of the Massachusetts Institute of Technology and the Hawaiian Volcano Research Association: January–March 1912. In: Bevens, D., Takahashi, T.J., Wright, T.L. (Eds.), The early serial publications of the Hawaiian Volcano Observatory. Hawaii Natural History Association, Hawaii, Vol. 1, pp. 73.

Jaggar, T.A., 1947. Origin and development of craters. Geol. Soc. Am. Mem. 21.

Lapple, C.E., 1950. Dust and mist collection. In: Perry, J.H. (Ed.), Chemical Engineers' Handbook, 3rd edn. McGraw Hill, New York.

Lawn, B.R., Wilshaw, T.R., 1975. Fracture of Brittle Solids. Cambridge University Press, Cambridge.

Lipman, P.W., Lockwood, J.P., Okamura, A.T., Swanson, D.A., Yamashita, K.M., 1985. Ground deformation associated with the 1975 magnitude 7.2 earthquake and resulting changes in activity of Kilauea volcano, Hawaii. US Geol. Surv. Prof. Pap. 1276.

Martel, S.J., Boger, W.A., in press. Geometry and mechanics of secondary fracturing around small three-dimensional faults in grantitic rock. J. Geophys. Res.

Macdonald, G.A., 1972. Volcanoes. Prentice-Hall, New Jersey.

Macdonald, G.A., Abott, A.T., Peterson, F.L., 1990. Volcanoes in the Sea. University of Hawaii Press, Honolulu, pp. 44–45.

Macdonald, G.A., Eaton, J.P., 1964. Hawaiian volcanoes during 1955. US Geol. Surv. Bull. 1171, 98–101.

Mastin, L.G., Pollard, D.D., 1988. Surface deformation and shallow dike intrusion processes at Inyo Craters, Long Valley, California. J. Geophys. Res. 93, 13221–13235.

Pollard, D.D., Delaney, P.T., Duffield, W.A., Endo, E.T., Okamura, A.T., 1983. Surface deformation in volcanic rift zones. Tectonophysics 94, 541–584.

Pollard, D.D., Segall, P., 1987. Theoretical displacements and stresses near fractures in rock: with applications to faults, joints, veins, dikes, and solution surfaces. In: Atkinson, B.K. (Ed.), Fracture Mechanics of Rock. Academic Press, London, pp. 277–349.

de Saint Ours, P., 1982. Structural map of the summit area of Kilauea volcano, Hawaii. US Geol. Surv. Misc. Field Studies Map, MF-1368.

Schultz, A.R., Aydin, A., 1990. Formation of interior basins associated with curved faults in Alaska. Tectonics 9, 1387–1407.

Scribner, C.W., Doerr, J.E., 1932. Exploring the Devil's Throat. Hawaii National Park Nature Notes 2, 23–26.

Senske, D.A., Schaber, G.G., Stofan, E.R., 1992. Regional topographic rises on Venus: geology of western Eistla Regio and comparison to Beta Regio and Atla Regio. J. Geophys. Res. 97, 13395–13420.

Stearns, H.T., 1926. The Keaiwa or 1823 lava flow from Kilauea volcano, Hawaii. J. Geol. 34, 336–351.

Stearns, H.T., Clark, W.O., 1930. Geology and water resources of the Kau District, Hawaii. US Geol. Surv. Water Supply Paper: 616.

Stone, J.B., 1926. The Keaiwa flow of 1823 Hawaii. Am. J. Sci. 11, 434–440, 5th series.

Swanson, D.A., Duffield, W.A., Fiske, R.S., 1976. Displacement of the south flank of Kilauea volcano: the result of forceful intrusion of magma into the rift zones. US Geol. Surv. Prof. Pap. 963.

Thomas, A.L., 1994. POLY3D: a three-dimensional, polygonal element, displacement discontinuity boundary element computer program with applications to fractures, faults, and cavities in the earth's crust. M.S. thesis, Stanford University.

Walker, G.P.L., 1987. The dike complex of Koolau volcano, Oahu: Internal structure of a Hawaiian rift zone. In: Decker, R.T., Wright, T.L., Stauffer, P.H. (Eds.), Volcanism in Hawaii. US Geol. Surv. Prof. Pap. 1350, 961–993.

Walker, G.P.L., 1988. Three Hawaiian calderas: an origin through loading by shallow intrusions?. J. Geophys. Res. 93, 14773–14784.

Whitfield, P., 1980. Western cone crater, Hawaii, 19 and 20 December, 1979. Cascade Caver 19, 49.

Wilkes, C., 1845. Narrative of the United States Exploring Expedition during the years 1838, 1839, 1840, 1841, and 1842, Vol. 4. Lea and Blanchard, Philadelphia, 180 pp.